JPE 12-5-13

http://dx.doi.org/10.6113/JPE.2012.12.5.800

Novel Control Method for a Hybrid Active Power Filter with Injection Circuit Using a Hybrid Fuzzy Controller

MinhThuyen Chau[†*], An Luo[*], Zhikang Shuai[*], Fujun Ma[*], Ning Xie[*], and VanBao Chau[**]

[†*]College of Electrical and Information Engineering, Hunan University, Changsha, China
[**]Faculty of Electrical Engineering, Ho Chi Minh University of Industry, Ho Chi Minh City, Viet Nam

Abstract

This paper analyses the mathematical model and control strategies of a Hybrid Active Power Filter with Injection Circuit (IHAPF). The control strategy based on the load harmonic current detection is selected. A novel control method for a IHAPF, which is based on the analyzed control mathematical model, is proposed. It consists of two closed-control loops. The upper closed-control loop consists of a single fuzzy logic controller and the IHAPF model, while the lower closed-control loop is composed of an Adaptive Network based Fuzzy Inference System (ANFIS) controller, a Neural Generalized Predictive (NGP) regulator and the IHAPF model. The purpose of the lower closed-control loop is to improve the performance of the upper closed-control loop. When compared to other control methods, the simulation and experimental results show that the proposed control method has the advantages of a shorter response time, good online control and very effective harmonics reduction.

Key words: ANFIS, Compensation reactive power, Fuzzy logic, Harmonics, Hybrid active power filter, Hybrid fuzzy

I. INTRODUCTION

Nowadays, the increasing use of nonlinear loads is one of the main causes of harmonics in power systems. In order to solve the harmonic problem, a passive power filter (PPF) [1], [2] is often used. However, it has many disadvantages (resonance, instability, mistuning, etc.). From here, the Active Power Filter (APF) [3], [4] appears to be a viable solution for eliminating harmonic current and achieving reactive power compensation. It is often parallel-connected with a non-linear load. Nevertheless, it is limited due to its high cost, low-power capacity and the fact that it is difficult to use in high-voltage grids. Another solution for the harmonic problem is to adopt a hybrid active power filter (HAPF) [5], [6]. The HAPF is the combination of an active power filter and a passive power filter. The aim of the HAPF design is to reduce the APF capacity. In addition, the HAPF inherits the advantages of both passive and active power filters. The IHAPF is a novel HAPF with injection circuit. It has great promise in reducing harmonics with a relatively low capacity APF.

For harmonic current tracking control, there are usually two ways: one includes conventional control methods, such as PI control, hysteresis control, deadbeat control, etc; the other includes intelligent control methods, such as fuzzy control, PI-fuzzy control, neural network control, etc. The hysteresis control is characterized by its simplicity and fast response, but its disadvantage is that it depend on a widely varying switching frequency [7]. The conventional PI control has many advantages such as a simple structure and ease of use [8]. However, the K_P, K_I parameters are fixed during the whole control process. Therefore, with fast variable nonlinear loads, the dynamic response of the PI controller is not good. With the fuzzy logic controllers, using the Mamdani Fuzzy Inference System is the most popular. It is conceptually easy to understand, flexible and it can be combined with conventional control techniques [9]-[14]. However, the input-output memberships are fixed and cannot be learned during the whole control process and its parameters depend on experience. If the controller uses a neural network, the result relies on the training algorithm [15], [16]. The neural network

Manuscript received Sep. 12, 2011; revised Jun. 20, 2012
Recommended for publication by Associate Editor Kyeon Hur.
[†]Corresponding Author: ttcmt060677@yahoo.com.vn
Tel: +86-15207494968, Fax: +86-0731-88823700, Hunan University
[*]College of Electrical and Information Engineering, Hunan University, China
[**]Faculty of Electrical Engineering, Ho Chi Minh University of Industry, Viet Nam

controller can learn but the response is relatively slow and the transient time is large.

Another control method used for harmonic current tracking is an Adaptive network based fuzzy inference system (ANFIS) [17]. The ANFIS uses linguistic variables to build a databases in the form of the fuzzy if-then rules of Takagi and Sugeno's type [18]. The ANFIS uses techniques such as hybrid or back propagation learning rules to determine the input membership functions. Flowing that, the input membership functions after learning will give the desired results in the output. However, the ANFIS controller also has some drawbacks such as the fact that: it has a single output, all of the output membership functions must be the same type (they must be either be linear or constant), different rules cannot share the same output membership function, have unity weight for each rule, based on the given learning data sets. Therefore, if the system only uses a single ANFIS controller then it is very difficult to achieve good results.

In short, the above mentioned control methods aim at either the time-domain response or the frequency response characteristics of the process, which is not suitable for online control.

This paper presents a novel control method for a IHAPF using a hybrid fuzzy controller, which consists of three control units: a single fuzzy logic controller, an ANFIS and a NGP. The ANFIS unit is regulated online by the NGP regulator. The NGP regulator consists of the predictive neural network model and the generalized predictive control (GPC) criterion. This control method can improve the performance of the single fuzzy logic controller and the ANFIS controllers. A single fuzzy logic controller for the IHAPF is presented first. At the same time, the output signals of the ANFIS controller are added to the output of a single fuzzy logic controller. Therefore, the output of the proposed controller will be changed and the purpose is to reduce the response time and to minimize the error in the steady-state. This new control method is very suitable for nonlinear controls, and it is able to achieve online control very well.

This paper is organized as follows: Section I gives an introduction of the former research on the IHAPF. The mathematical model and control strategies of the IHAPF are highlighted in Section II. Section III proposes the single fuzzy logic control scheme for the IHAPF. Section IV represents the proposed control method for the IHAPF. Simulation and experimental results are presented in Section V, and Section VI draws some conclusions.

II. MATHEMATICAL MODEL AND CONTROL STRATEGIES OF THE IHAPF

The topology of the IHAPF is proposed as shown in Fig. 1.

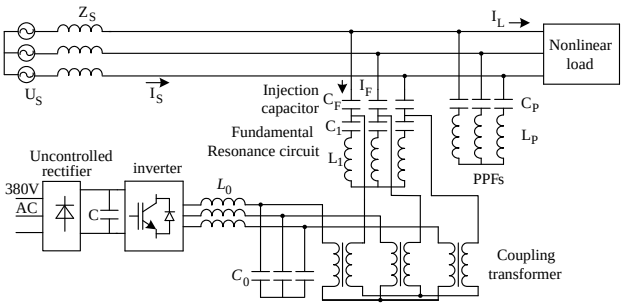

Fig. 1. Topology of the IHAPF.

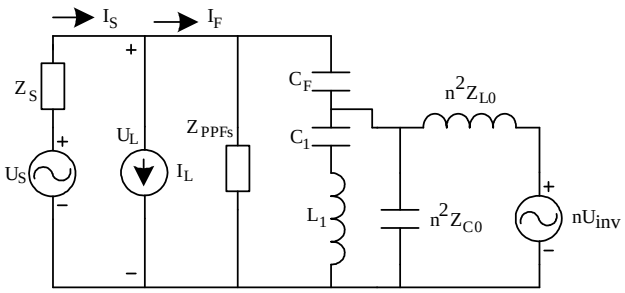

Fig.2. Single-phase equivalent circuit of IHAPF.

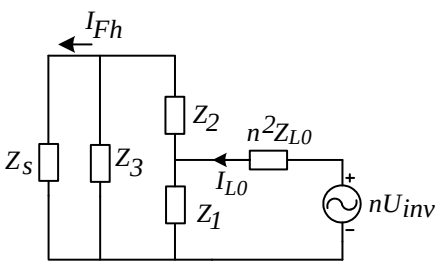

Fig. 3. Single-phase equivalent circuit when only the U_{inv} is considered.

Where: U_s and Z_s are the supply voltage and the equivalent impedance of the grid, respectively. C_F, C_1, L_1, C_P, L_P, L_0, and C_0 are the injection capacitor, the fundamental resonance capacitor, the fundamental resonance inductor, the PPF capacitor, the PPF inductor, the output filter inductor and the output filter capacitor, respectively.

A single-phase equivalent circuit of the IHAPF is shown in Fig. 2.

A single-phase equivalent circuit when only the voltage source inverter U_{inv} is considered (U_s =0; I_L =0) is shown in Fig. 3.

where:

$$\begin{cases} Z_s = R_s + L_s s \\ Z_1 = Z_{L_1C_1} // n^2 Z_{C0} \\ Z_2 = \dfrac{1}{C_F s} \\ Z_{L0} = R_0 + L_0 s \\ Z_3 = Z_{PPFs} \end{cases} \quad (1)$$

From Fig. 3, the harmonic current injection into the grid by the IHAPF can be calculated:

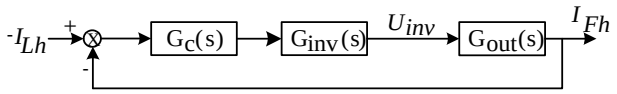

Fig. 4. Control strategy based on load harmonic current detection.

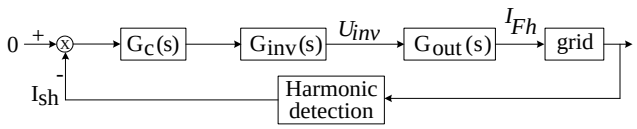

Fig. 5. Control strategy based on source harmonic current detection.

$$I_{Fh} = \frac{nU_{inv}.Z_1.Z_3}{n^2 Z_{L0}[Z_3(Z_1+Z_2)+Z_s(Z_1+Z_2+Z_3)]+Z_1(Z_2Z_s+Z_2Z_3+Z_3Z_s)} \quad (2)$$

Equation (2) indicates that, compensation harmonic current is determined by the voltage source inverter U_{inv} and the response of the output circuit $G_{out}(s)$.

Suppose that the transfer function of the compensation harmonic current I_{Fh} to the inverter output voltage U_{inv} is $G_{out}(s)$.

$$G_{out}(s) = \frac{I_{Fh}}{U_{inv}} = \frac{nZ_1.Z_3}{n^2 Z_{L0}[Z_3(Z_1+Z_2)+Z_s(Z_1+Z_2+Z_3)]+Z_1(Z_2Z_s+Z_2Z_3+Z_3Z_s)} \quad (3)$$

The parameters of the output circuit are fixed during the whole control process. The voltage source inverter (VSI) in the IHAPF is controlled as a voltage source. Following this, there are two control strategies for U_{inv} :

A. Control Strategy Based On Load Harmonic Current Detection

The control strategy based on load harmonic current detection is shown in Fig. 4.

According to Fig. 4, the following is obtained:

$$U_{inv} = \frac{G_c(s).G_{inv}(s).I_{Lh}}{1-G_c(s).G_{inv}(s).G_{out}(s)} = K_1(s).I_{Lh} \quad (4)$$

where $G_c(s), G_{inv}(s)$ are the transfer functions of the controller and the voltage source inverter, respectively.

$$K_1(s) = \frac{G_c(s).G_{inv}(s)}{1-G_c(s).G_{inv}(s).G_{out}(s)} \quad (5)$$

B. Control Strategy Based On Source Harmonic Current Detection

The control strategy based on source harmonic current detection is shown in Fig. 5.

$$U_{inv} = G_c(s).G_{inv}(s)(-I_{sh}) = K_2(s).I_{sh} \quad (6)$$

$$K_2(s) = -G_c(s).G_{inv}(s) \quad (7)$$

In this paper, the control strategy based on load harmonic current detection is applied.

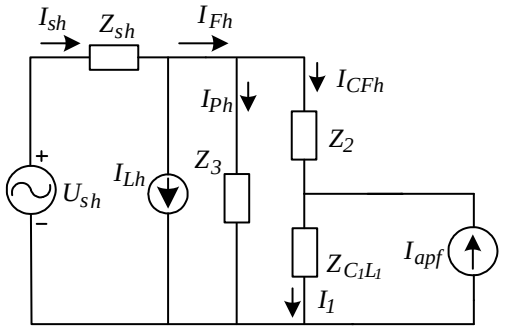

Fig. 6. Single-phase equivalent circuit with the effect of a harmonic source.

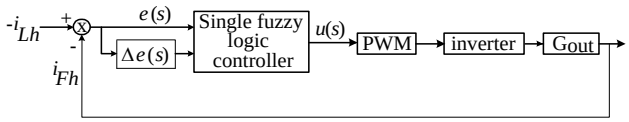

Fig. 7. Configuration of the control scheme using the single fuzzy logic controller.

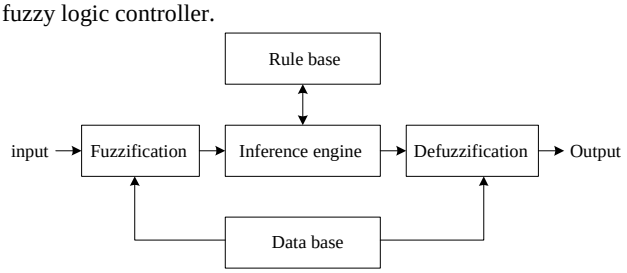

Fig. 8. Structure of a fuzzy logic controller.

A single-phase equivalent circuit with the effect of a harmonic source is shown in Fig. 6.

Where: $I_{apf}=K_1 I_{Lh}$ is output current of the APF.

$$\begin{cases} I_{sh} = I_{Lh} + I_{Fh} \\ I_1 = I_{apf} + I_{CFh} \\ I_{Fh} = I_{Ph} + I_{CFh} \\ I_{sh}Z_{sh} + I_{Ph}Z_3 = U_{sh} \\ I_{CFh}Z_2 + I_1 Z_{C1L1} = I_{Ph}Z_3 \end{cases} \quad (8)$$

From (8), I_{sh} can be calculated as:

$$I_{sh} = \frac{(Z_2 + Z_{C1L1} - K_1 Z_{C1L1})Z_3 I_{Lh}}{(Z_2 + Z_{C1L1})(Z_3 + Z_{sh}) + Z_3 Z_{sh}} \quad (9)$$

Equation (9) indicates that it is possible to eliminate the influence of the load harmonic current and make the supply harmonic current as low as possible if K_1 is large enough.

III. SINGLE FUZZY LOGIC CONTROL SCHEME FOR THE IHAPF

First, only a single fuzzy logic controller for the IHAPF is used. The configuration of the control scheme for the IHAPF using the single fuzzy logic controller is presented in Fig. 7.

The structure of the single fuzzy logic controller can be seen in Fig.8.

Where: *e(s)* and *Δe(s)* are the inputs and *u(s)* is the output of

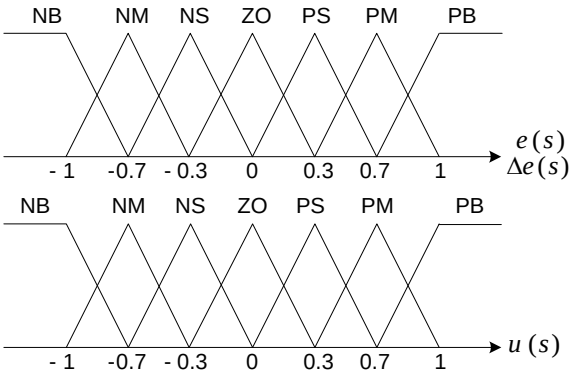

Fig. 9. Membership functions of the fuzzy variable.

TABLE I

ADJUSTING RULES OF THE SINGLE FUZZY LOGIC CONTROLLER

u(s)		*Δe(s)*						
		NB	NM	NS	ZO	PS	PM	PB
e(s)	NB	NB	NB	NB	NB	NB	NM	NM
	NM	NB	NB	NB	NM	NM	NM	NS
	NS	NB	NM	NM	NS	PS	PM	PM
	ZO	NM	NS	NS	ZO	PS	PS	PM
	PS	NM	NM	NS	PS	PM	PM	PB
	PM	PS	PM	PM	PM	PB	PB	PB
	PB	PM	PB	PB	PB	PB	PB	PB

the single fuzzy logic controller, and they can be written as:

$$e(s) = -I_{Lh}(s) - I_{Fh}(s)$$

$$\Delta e(s) = e(s) - e(s-1)$$

e(s) and *Δe(s)* are variable values from a real system. To convert these variable values into linguistic variables, the following seven fuzzy sets are chosen, as shown in Fig. 9: Positive Big (PB), Positive Medium (PM), Positive Small (PS), Zero (ZO), Negative Small (NS), Negative Medium (NM) and Negative Big (NB).

Membership functions are stored in the database. The linguistic control rule is the core of the fuzzy control, which is determined in the following:

1) if the values of *e(s)* and *Δe(s)* are positive, then *u(s)* is positive.
2) if the values of *e(s)* and *Δe(s)* are negative, then *u(s)* is negative.
3) if the values of *e(s)* and *Δe(s)* are zero, then *u(s)* is zero.
4) if the value of *e(s)* is zero and the value of *Δe(s)* is positive, then *u(s)* is positive.
5) if the value of *e(s)* is zero and the value of *Δe(s)* is negative, then *u(s)* is negative.

As a result, the adjusting rules of the single fuzzy logic controller can be obtained as in Table I.

This paper uses the *min–max* inference method to obtain the corresponding fuzzy set. The center of gravity method is used to defuzzify the fuzzy variable into the physical domain.

TABLE II

SIMULATION PARAMETERS WITH THE FUZZY LOGIC CONTROL SCHEME

$-I_{Lh}(s)$	$I_{Fh}(s)$	*e(s)*	*u(s)*	*switching*
80.2	100.0	-19.8	20.32	0
-145.3	-99.4	-45.9	-43.36	0
-80.0	-75.6	-4.4	-17.00	0
-115.0	-95.0	-20.0	-43.36	0
-140.0	-120	-20.0	-43.36	0
71.5	65.2	6.3	17.00	1
30.0	28.0	2.0	17.00	1
135.0	110.0	25.0	40.32	1
115.0	100.0	15.0	36.00	1
90.0	80.0	10.0	36.00	1
145.0	98.5	46.5	40.84	1

$$u(s) = \frac{\sum_{i=1}^{n} \mu_S\big(e(s), \Delta e(s)\big) u(s)}{\sum_{i=1}^{n} \mu_S\big(e(s), \Delta e(s)\big)} \tag{10}$$

The output of the single fuzzy logic controller is used in the generation of the PWM reference signal of the voltage source inverter. The switching signal is generated by means of comparing a reference signal with a carrier signal. The amplitude of the carrier signal is set between -100 and 100, and the frequency is 10 kHz. The output signal of the voltage source inverter will flow into the grid through the output circuit.

Simulation results with the single fuzzy logic controller are shown in Fig. 14(b). From this figure, consider its parameters at the peak positive and peak negative points of the error as in Table II. From the obtained parameters in Table II, it can be seen that: the single fuzzy logic controller based IHAPF has some good uncontrollable regions, and that the error value between the requested value ($-I_{Lh}$) and the compensation value (I_{Fh}) is large. For example: at the same value where *u(s)* is -43.36A, the requested values are -145.3A and 115.0A, but the compensation values are -99.4A and -95A, respectively. Or, when the requested value is 145.0A, the compensation value is 98.5A. Thus the error value is 46.5A. The cause of the error is that the membership functions and the parameters of the single fuzzy logic controller are established based on experience and are fixed during the whole control process.

IV. PROPOSED CONTROL METHOD FOR IHAPF

According to the above analysis, the single fuzzy logic controller for the IHAPF has some disadvantages. Moreover, when the load changes, the membership functions and fuzzy rules of the single fuzzy logic controller are not suitable. These disadvantages can be solved by using an ANFIS controller and a NGP regulator. The goal of the predictive neural network model is to determinate a structure that online

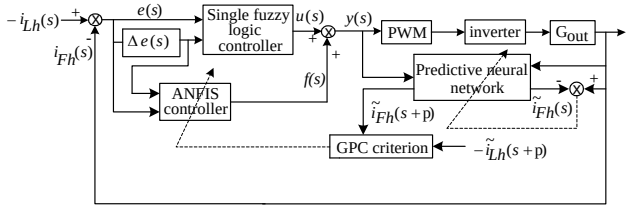

Fig. 10. Configuration of the proposed control method.

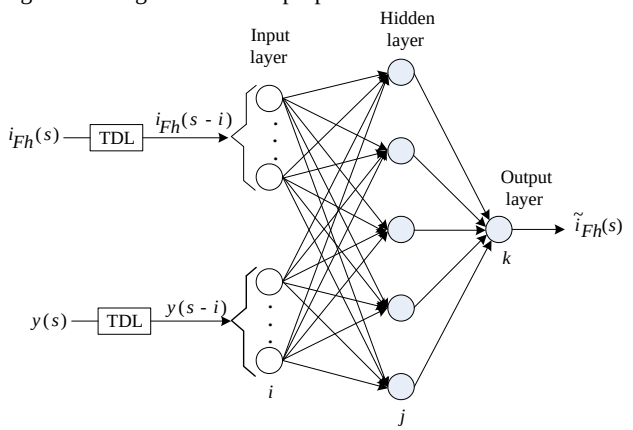

Fig. 11. Neural network structure.

emulates the nonlinear process of the IHAPF and makes the future values in the time *(s+p)* of the IHAPF. These future values will be sent to the GPC criterion together with the future reference values. The minimization of the GPC criterion will make an output value in the time *(s+p)* as *y(s+p)*. This output will regulate the parameters of the ANFIS to generate the best optimal value *f(s)*. Accordingly, *y(s)=u(s)+f(s)* will be the best optimal output of the proposed controller. The purpose of the proposed control scheme is to receive a minimum steady-state error with a shorter dynamic response time. The configuration of the proposed control method is presented in Fig. 10.

Where: *u(s)* is the output from the single fuzzy logic controller, which can not be the optimal output and *f(s)* is an incremental form from the ANFIS controller.

The neural network model used here is a three layer feed-forward neural network with a time-delayed structure that has a hyperbolic tangent activation function in the hidden layer and a linear activation function in the output layer. The structure of the neural network is shown in Fig. 11. The inputs to this neural network consist of *u(s)* and $I_{Fh}(s)$ with their corresponding delay nodes *u(s-i)* and $I_{Fh}(s-i)$. The neural network model uses the previous inputs and the previous IHAPF outputs to predict the future values of the IHAPF output. These predicted output values are used in the generalized predictive control (GPC) criterion.

The equations for this neural network model are:

$$\tilde{i}_{Fh}(s)=\sum_{j=1}^{hid}\omega_{jk}.f_j\left(net_j(s)\right)+b_k \qquad (11)$$

$$net_j(s)=\sum_{i=1}^{n_u}\omega_{j,i}y(s-i)+\sum_{i=1}^{n_{I_{Fh}}}\omega_{j,n_u+i}I_{Fh}(s-i)+b_j \qquad (12)$$

where f_j is the transfer function of the hidden neural *j*, ω_{jk} and b_k are the weights and the bias of the hidden to the output layers, $\omega_{j,i(nu+i)}$ and b_j are the weights and the bias of the input to the hidden layers, and $net_j(s)$ is the summation of all of the products between the inputs and the input to the hidden weights in the input layer.

From (11), the predict future output value of the IHAPF from the current time *(s)* to the future time *(s+p)* can be written as:

$$\tilde{i}_{Fh}(s+p)=\sum_{j=1}^{hid}\omega_{jk}.f_j\left(net_j(s+p)\right)+b_k \qquad (13)$$

The model predictive control method is based on the receding horizon technique. The neural network model predicts the IHAPF response over a specified time horizon. The predictions are used by a numerical optimization program to determine the control signal *y(s)* that minimizes the following performance criterion over the specified horizon.

Consider the cost function of the GPC criterion:

$$J=\frac{1}{2}\sum_{k=N_1}^{N_2}\left[-\tilde{i}_{Lh}(s+p)-\tilde{i}_{Fh}(s+p)\right]^2+\frac{1}{2}\sum_{k=1}^{N_u}\lambda_k\left[\Delta y(s)\right]^2 \qquad (14)$$

Where:

N_1: the minimum cost prediction horizon

N_2: the maximum cost prediction horizon

N_u: the length of the control horizon

$-\tilde{i}_{Lh}(s+p)$ is the desired response of I_{Lh} at the time *(s+p)*.

$\tilde{i}_{Fh}(s+p)$ is the predicted output of the IHAPF at time *(s+p)*.

Δy(.) is the control increment variable to minimize the objective function *J*.

λ_k is the selected weighing factor value, $\lambda_k>0$.

Based on the gradient descent method, the control variable *y(s)* is obtained from the optimization of cost function (14):

$$\begin{aligned}y(s)&=y(s-1)+\Delta y(s)\\&=y(s-1)+\eta\left(G^T(s).\left(-\tilde{i}_{Lh}(s+p)-\tilde{i}_{Fh}(s+p)\right)-\lambda_k\Delta y(s)\right)\end{aligned} \qquad (15)$$

where:

$$G(s)=\left[\frac{\partial\tilde{i}_{Fh}(s+1)}{\partial y(s)}\quad\frac{\partial\tilde{i}_{Fh}(s+2)}{\partial y(s)}\ldots\frac{\partial\tilde{i}_{Fh}(s+N_2)}{\partial y(s)}\right]^T \qquad (16)$$

When $\dfrac{\partial\tilde{i}_{Fh}(s+p)}{\partial y(s)}=\dfrac{\partial\left(\sum_{j=1}^{hid}\omega_{jk}.f_j(net_j(s+p))+b_k\right)}{\partial y(s)}$

η is learning rate.

From (15), the increment control *Δy(s)* can be calculated as follows:

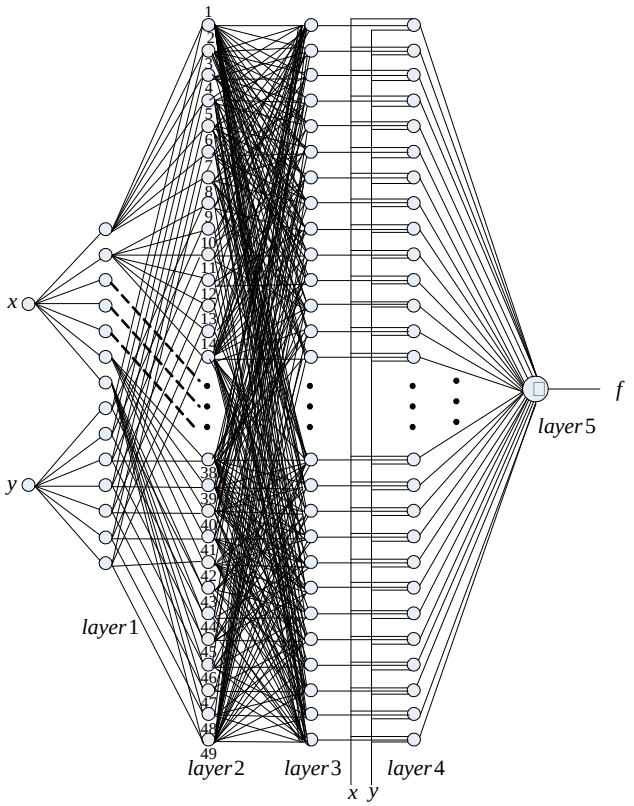

Fig. 12. Structure of ANFIS.

TABLE III

ADJUSTING RULES OF THE ANFIS CONTROLLER

f(s)		*Δe(s)*						
		NB	NM	NS	ZO	PS	PM	PB
e(s)	NB	f1	f2	f3	f4	f5	f6	f7
	NM	f8	f9	f10	f11	f12	f13	f14
	NS	f15	f16	f17	f18	f19	f20	f21
	ZO	f22	f23	f24	f25	f26	f27	f28
	PS	f29	f30	f31	f32	f33	f34	f35
	PM	f36	f37	f38	f39	f40	f41	f42
	PB	f43	f44	f45	f46	f47	f48	f49

$$\Delta y(s) = \frac{\eta}{1+\eta\lambda_k} G^T(s).\left(-\tilde{i}_{Lh}(s+p) - \tilde{i}_{Fh}(s+p)\right) \quad (17)$$

Setting $y(s) - u(s) = f_r(s)$ yields the reference signal to regulate the parameters of the ANFIS controller. The ANFIS outputs are trained by training the data sets $f_r(s)$, and their results are added to the output of the single fuzzy logic controller.

The architecture of the ANFIS is shown in Fig. 12. Here: x and y are the inputs (*e(s)* and *Δe(s)*), respectively, while the output is *f(s)*.

Suppose that the rules are Takagi and Sugeno's type [18].

If x is A_1 and y is B_1 then the *output* is $f_1 = p_1x + q_1y + r_1$.

If x is A_2 and y is B_2 then the *output* is $f_2 = p_2x + q_2y + r_2$.

where A_i and B_j *are* the linguistic labels (Positive Big (PB), Positive Medium (PM), Positive Small (PS), Zero (ZO), Negative Small (NS), Negative Medium (NM) and Negative Big (NB)). p_i, q_i and r_i are .consequent parameters and i is the node number.

Layer1: every node i in this layer with a node function.

$$O_i^1 = \mu_{A_i(x)} \ , \quad O_j^1 = \mu_{B_j(x)} \quad (18)$$

O_i is the membership function of A_i and O_j is the membership function of B_j.

$$\mu_{A_i(x)} = 1 \Big/ 1 + \left[\left(\frac{x - c_i}{a_i}\right)^2\right] b_i \quad (19)$$

Where: a_i and b_i are the parameters which regulate the width of the curve and c_i locates the center of the curve.

Layer 2: every node in this layer multiplies the incoming signals and sends out the product.

$$\omega_i = \mu_{A_i(x)} . \mu_{B_i(y)}, \ i = 1, 2 \quad (20)$$

Layer 3: this node calculates the ratio of the i_{th} rule's firing strength to the sum of all rule's firing strengths:

$$\overline{\omega}_i = \omega_i / (\omega_1 + \omega_2), \ i = 1, 2... \quad (21)$$

Layer 4: this node multiplies the output of layer 3 with function f_i.

$$O_i^4 = \overline{\omega}_i . f_i = \overline{\omega}_i (p_i x + q_i y + r_i) \quad (22)$$

Where: $\overline{\omega}_i$ is the output of *layer 3* and p_i, q_i, r_i are the parameters set.

Layer 5: this is node calculates the overall output.

$$O_i^5 = \sum_i \overline{\omega}_i . f_i = \sum_i \omega_i f_i / \sum_i \omega_i \quad (23)$$

The adjusting rules of the *ANFIS* controller are described in Table III.

In this paper, the hybrid algorithm is used. It combines the gradient method and the least squares estimate (LSE) to update the parameters of the ANFIS controller. When the premise values of the system are fixed, the overall output can be expressed as:

$$f = \frac{\omega_1}{\omega_1 + \omega_2} f_1 + \frac{\omega_2}{\omega_1 + \omega_2} f_2 = \overline{\omega}_1 f_1 + \overline{\omega}_2 f_2$$
$$= \left(\overline{\omega}_1 x\right) p_1 + \left(\overline{\omega}_1 y\right) q_1 + \left(\overline{\omega}_1\right) r_1 + \left(\overline{\omega}_2 x\right) p_2 + \left(\overline{\omega}_1 y\right) q_2 + \left(\overline{\omega}_1\right) r_2 \quad (24)$$

The premise values are updated by the gradient descent method as follows:

$$a_i(t+1) = a_i(t) - \eta_a \frac{\partial E}{\partial a_i} \quad (25)$$

$$b_i(t+1) = b_i(t) - \eta_b \frac{\partial E}{\partial b_i} \quad (26)$$

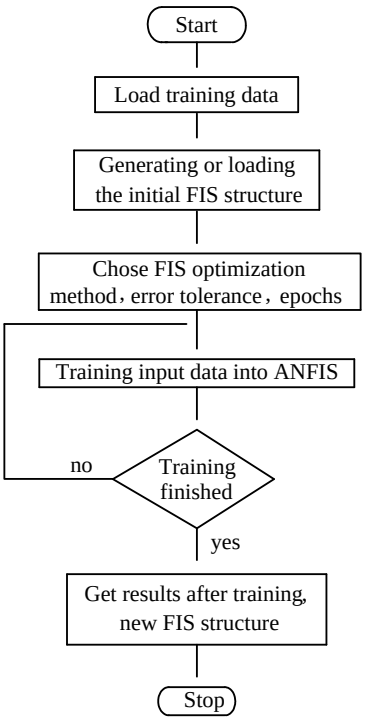

Fig. 13. Training methodology of ANFIS system.

$$\omega_i(t+1) = \omega_i(t) - \eta_\omega \frac{\partial E}{\partial \omega_i} \tag{27}$$

The cost function is defined as:

$$E = \frac{1}{2}(f - f_r)^2 \tag{28}$$

where f_r is the reference value and η_a is learning rate of a_i.

$$\frac{\partial E}{\partial a_i} = \frac{\partial E}{\partial f} \cdot \frac{\partial f}{\partial f_i} \cdot \frac{\partial f_i}{\partial \omega_i} \cdot \frac{\partial \omega_i}{\partial \mu_{ij}} \cdot \frac{\partial \mu_{Ai}}{\partial a_i} \tag{29}$$

$$\frac{\partial E}{\partial f} = (f - f_r) = e \tag{30}$$

$$f = \sum_{i=1}^{n} f_i \text{ , hence } \frac{\partial f}{\partial f_i} = 1 \tag{31}$$

$$f_i = \frac{\omega_i}{\sum_{i=1}^{n} \omega_i}(p_i x + q_i y + r_i) \tag{32}$$

$$\frac{\partial f_i}{\partial \omega_i} = \frac{(p_i x + q_i y + r_i) - f}{\sum_{i=1}^{n} \omega_i} \tag{33}$$

$$\omega_i = \prod_{j=1}^{m} \mu_{Aij} \text{ , hence } \frac{\partial \omega_i}{\partial \mu_{ij}} = \frac{\omega_i}{\mu_{Ai}} \tag{34}$$

Substituting (30), (31), (32), (33), (34) into (29), the following is obtained:

$$\frac{\partial E}{\partial a_i} = e. \frac{(p_i x + q_i y + r_i) - f}{\sum_{i=1}^{n} \omega_i} \cdot \frac{\omega_i}{\mu_{A_i}} \cdot \frac{\partial \mu_{Ai}}{\partial_{a_i}} \tag{35}$$

Similarly:

$$\frac{\partial E}{\partial b_i} = e. \frac{(p_i x + q_i y + r_i) - f}{\sum_{i=1}^{n} \omega_i} \cdot \frac{\omega_i}{\mu_{B_i}} \cdot \frac{\partial \mu_{Bi}}{\partial_{b_i}} \tag{36}$$

$$\frac{\partial E}{\partial \omega_i} = e.(p_i x + q_i y + r_i) \tag{37}$$

The training methodology of the ANFIS is shown in Fig. 13.

V. Simulation and Experimental Results

A. Simulation Results

Simulation results are implemented with MATLAB and PSIM software, where i_L, i_S, i_{Lh}, i_{Fh} and *error* represent the load current, the supply current, the load harmonic current, the compensation harmonic current into grid by the PPFs and the APF, and the error of compensation, respectively. Before compensation, the load current and the supply current are the same. The parameters of the system are represented as in the appendix. The neural network model is constructed and trained using the neural network toolbox predictive control with N_1=1; N_2=7; N_u=2 and λ=0.05.

Fig. 14 shows the dynamic response of the IHAPF when the different controllers are adopted. At t=0.2s the system is connected by the PPFs and the APF. Fig.14.(a) shows the dynamic response of the IHAPF when the conventional PI controller is used. The error can be reduced to ±50A from ±200A in 0.1s, but there is an obvious steady-state error at (0.3s-0.6s). All the same, the THD is reduced to 6.4% from 28.24%. Fig.14.(b) shows the dynamic response of the IHAPF when the single fuzzy logic controller is used. The error can be reduced to ±30A from ±200A in 0.1s, but there is an obvious steady-state error at (0.3s-0.6s). All the same, the THD is reduced to 5.72% from 28.24%. Fig.14.(c) shows the dynamic response of the IHAPF when the proposed controller is used. The error can be reduced to ±20A in 0.1s, and the steady-state compensation is ±7A in (0.5s-0.6s). The THD is reduced to 2.89% from 28.24%. At t=0.6s, the THD of the load increases to 34% from 28.24%. When the conventional PI controller is used, the error increases to ±70A from ±50A in 0.1s, but there is an obvious steady-state error at (0.7s-1.0s). All the same, the THD increases to 9.36% from 6.4%. When the single fuzzy logic controller is used, the error increases to ±50A from ±30A in 0.1s, but there is an obvious steady-state error at (0.7s-1.0s). All the same, the THD increases to 8.28% from 5.72%. When the proposed controller is used, the error increases to ±15A from ±7A in 0.1s. In the steady-state compensation, the error can be reduced to ±10A in (0.8s-1.0s), and the THD is increased to 3.58% from 2.89%.

Fig. 15 shows the frequency spectrum of the supply current i_s when the different controllers are used.

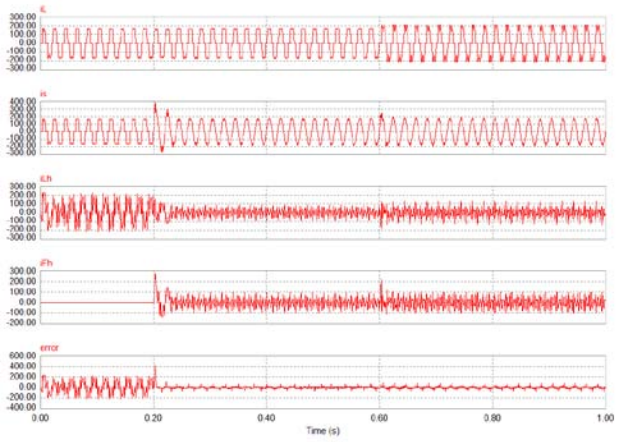

(a)

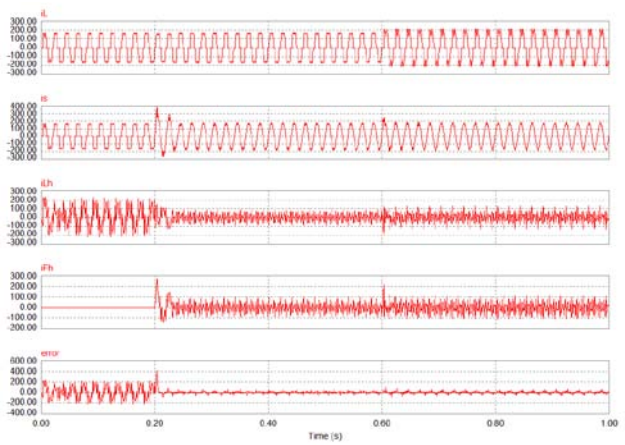

(b)

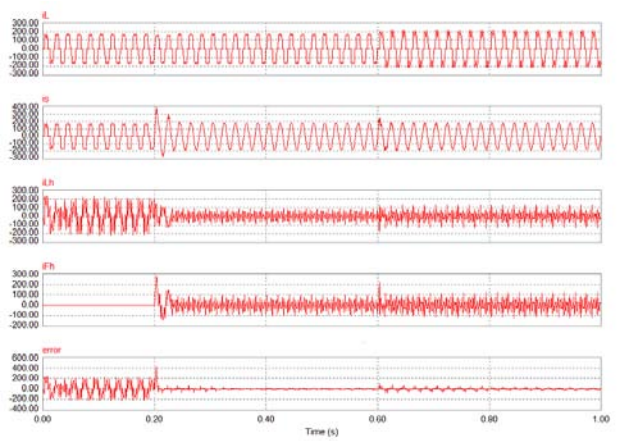

(c)

Fig. 14. Dynamic response of the IHAPF with different controllers. (a) Simulation results with the conventional PI controller. (b) Simulation results with the single fuzzy logic controller. (c) Simulation results with the proposed controller.

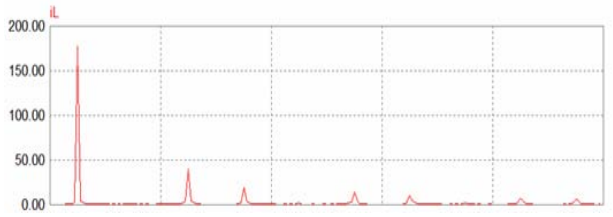

(a)

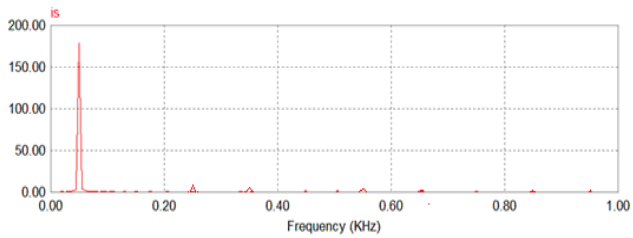

(b)

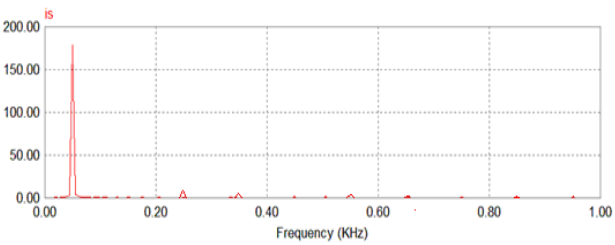

(c)

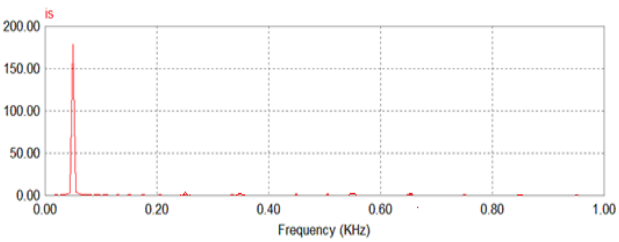

(d)

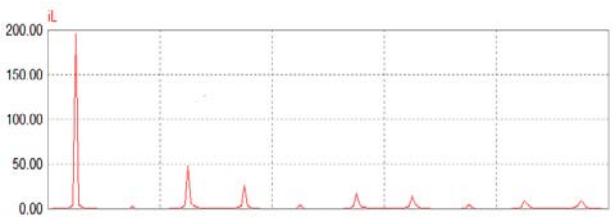

(e)

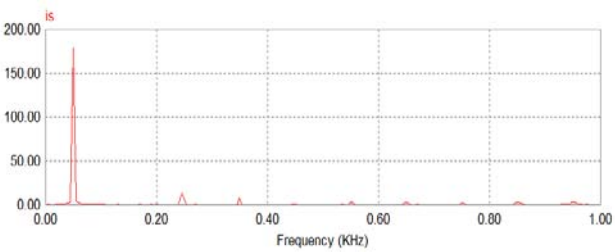

(f)

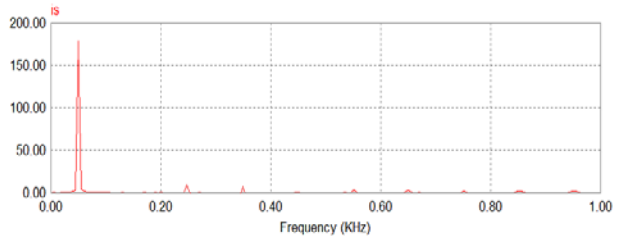

(g)

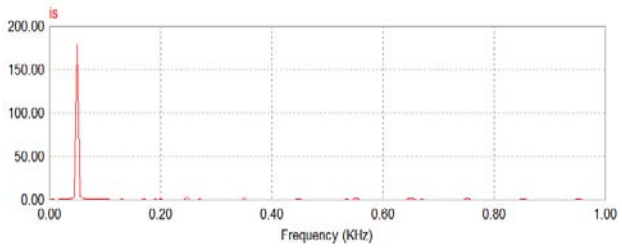

(h)

Fig. 15. Frequency spectrum of the supply current when the different control methods are used. (a) Frequency spectrum of the supply current before compensation in (0.2s-0.6s). (b) Frequency spectrum of the supply current after compensation with the conventional PI control method in (0.2s-0.6s). (c) Frequency spectrum of the supply current after compensation with the single fuzzy logic control method in (0.2s-0.6s). (d) Frequency spectrum of the supply current after compensation with the proposed control method in (0.2s-0.6s). (e) Frequency spectrum of the supply current before compensation in (0.6s-1.0s). (f) Frequency spectrum of the supply current after compensation with the conventional PI control method in (0.6s-1.0s). (g) Frequency spectrum of the supply current after compensation with the single fuzzy logic control method in (0.6s-1.0s). (h) Frequency spectrum of the supply current after compensation with the proposed control method in (0.6s-1.0s).

Table IV shows the summarization of the frequency spectrum of the load and supply currents. Table V shows a comparison of the supply current THD and the power factor. From Fig. 14, Fig. 15, Table IV and Table V, it can be seen that the proposed controller exhibits much better performance than the conventional PI and the single fuzzy logic controller in terms of reducing harmonics and a shorter dynamic response time.

B. Experimental results

In order to demonstrate that the proposed control method in this paper is better than the conventional PI and single fuzzy logic control methods, laboratory experiments have been implemented on a prototype of the IHAPF. A DSP-2812M is used on the controller board to implement the control methods. The system parameters are listed in the appendix. The IHAPF and the DSP-based controller are shown in Fig. 16. The experimental results are shown in Fig. 17 and Fig. 18. They prove that with the proposed control method the supply current changes from a distorted wave to a nearly ideal sinusoidal wave. In addition it has a shorter response time and is very effective in reducing harmonics.

TABLE IV

SUMMARIZATION OF FREQUENCY SPECTRUM OF THE LOAD AND SUPPLY CURRENTS

When the load doesn't changes (t=0.2s-0.6s)

Harmonic order	i_L(A)	i_s(A)		
		PI controller	Single fuzzy controller	Proposed controller
1st	177	178	178	178
5th	39.5	7.8	7.15	3.1
7th	19.0	5.8	5.42	2.7
11th	14.5	4.3	3.8	2.4
13th	9.81	2.9	2.5	2.0
17th	7.5	1.62	1.3	0.8
19th	6.27	1.32	1.02	0.58

When the load changes (t=0.6s-1s)

Harmonic order	i_L(A)	i_s(A)		
		PI controller	Single fuzzy controller	Proposed controller
1st	195	178	178	178
5th	47.9	11.7	10.1	4.15
7th	26.1	8.02	7.25	3.25
11th	17.1	6.2	5.6	2.9
13th	14.4	5.2	4.5	2.0
17th	8.98	2.6	2.3	0.8
19th	8.5	2.2	2.1	0.8

TABLE V

COMPARISON OF SUPPLY CURRENT THD AND POWER FACTOR

Time(s)	Control methods	THD%	cosφ
Before compensation (0s-0.2s)		28.24	0.85
After compensation (0.5-0.6s)	Conventional PI method	6.4	0.99
	Single fuzzy logic method	5.72	0.99
	Proposed method	2.89	0.99
After compensation (0.9-1s) (At t=0.6-1s, THD of load changes from 28.24% to 34%)	Conventional PI method	9.36	0.97
	Single fuzzy logic method	8.28	0.97
	Proposed method	3.58	0.97

Fig. 16. Local equipment of IHAPF and DSP-based controller.

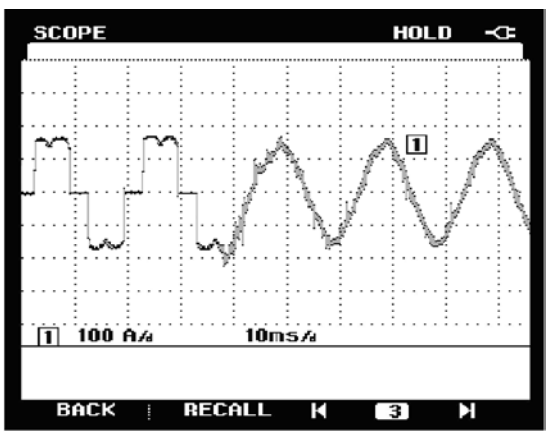

(a)

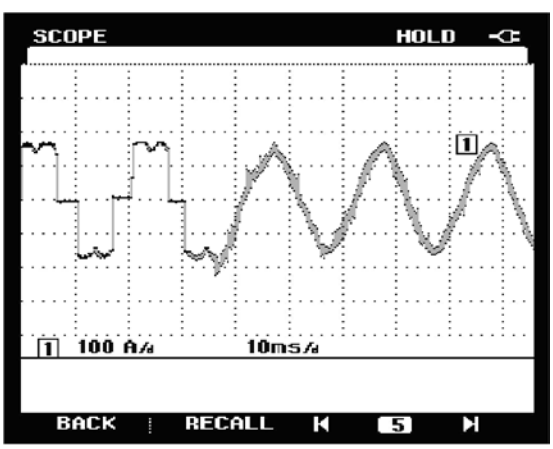

(b)

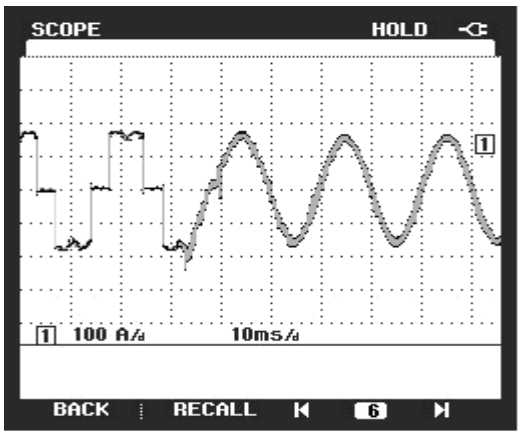

(c)

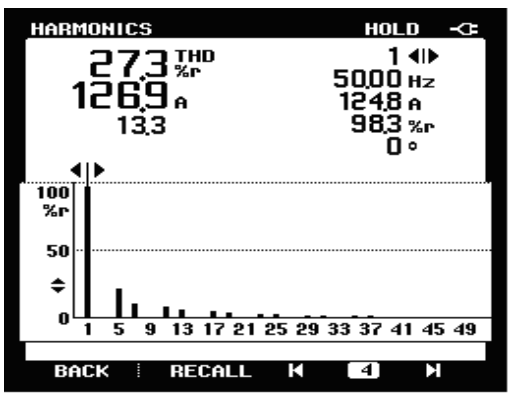

(d)

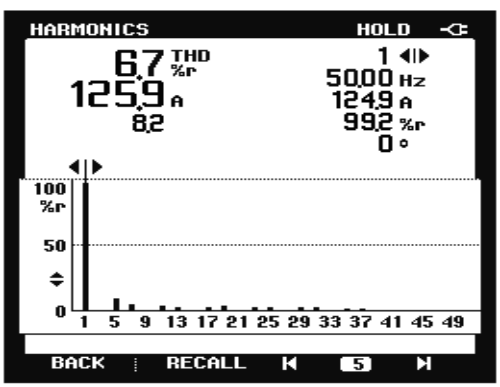

(e)

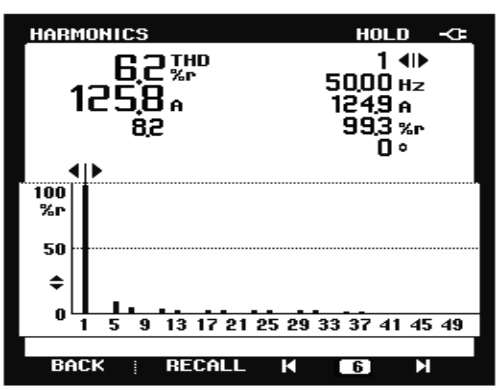

(f)

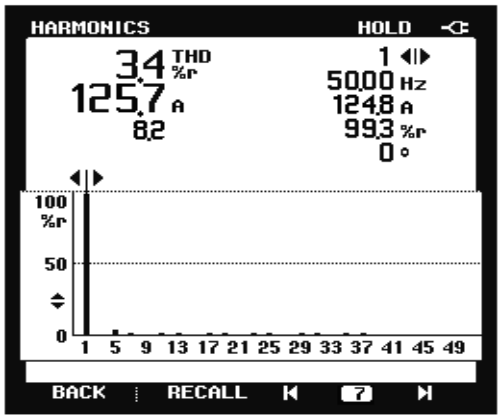

(g)

Fig. 17. Experimental results before the load change. (a) Dynamic response of the supply current when the conventional PI controller is used. (b) Dynamic response of the supply current when the single fuzzy logic controller is used. (c). Dynamic response of the supply current when the proposed controller is used. (d) Frequency spectrum of supply current before compensation. (e) Frequency spectrum of supply current after compensation with the conventional PI controller. (f) Frequency spectrum of supply current after compensation with the single fuzzy logic controller. (g) Frequency spectrum of supply current after compensation with the proposed controller.

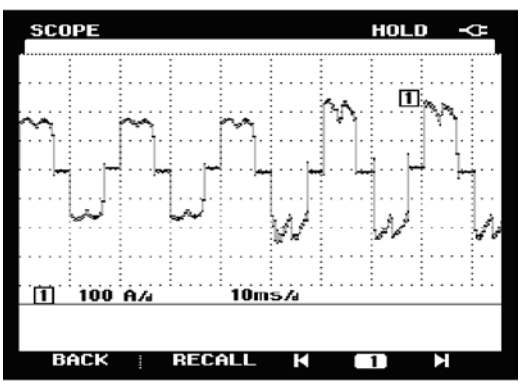

(a)

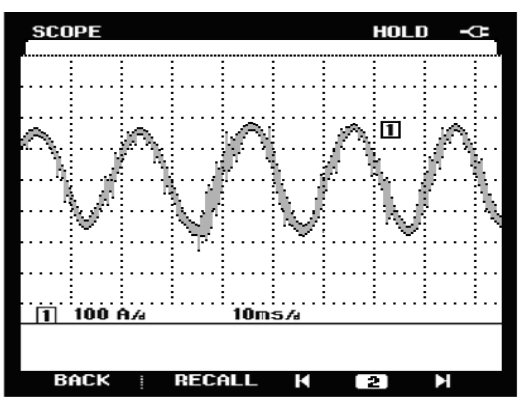

(b)

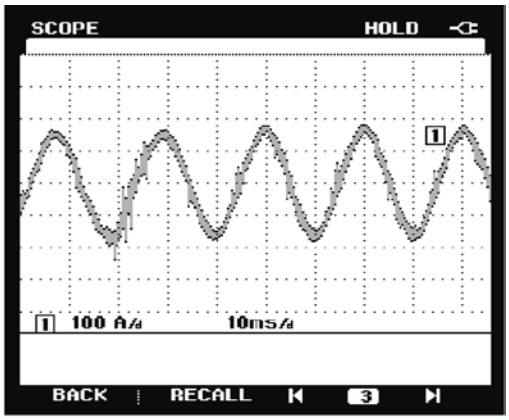

(c)

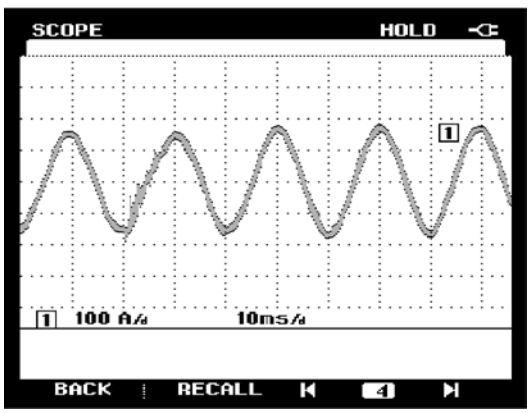

(d)

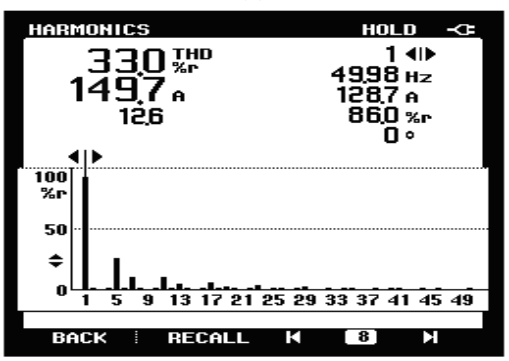

(e)

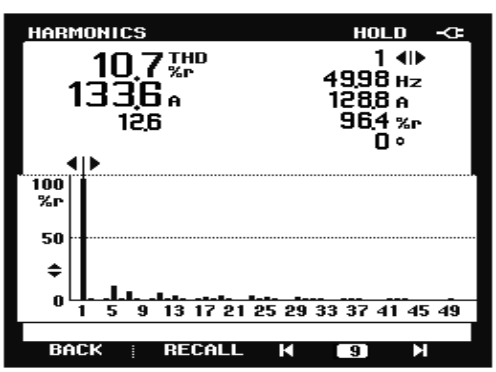

(f)

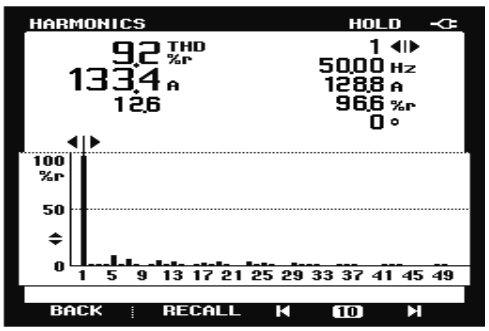

(g)

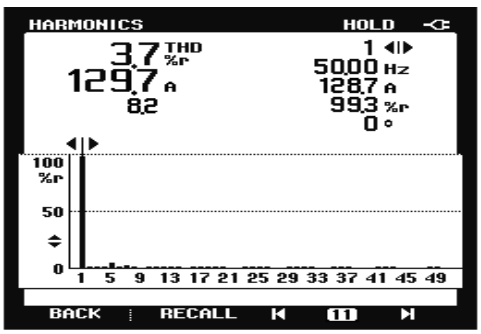

(h)

Fig. 18. Experimental results after the load change. (a) Dynamic response of the load current when load changing. (b) Dynamic response of the supply current with the conventional PI controller. (c) Dynamic response of the supply current with the single fuzzy logic controller. (d) Dynamic response of the supply current with the proposed controller. (e). Frequency spectrum of load current after changed. (f) Frequency spectrum of supply current after compensation with the conventional PI controller. (g) Frequency spectrum of supply current after compensation with the single fuzzy logic controller. (h) Frequency spectrum of supply current after compensation with the proposed controller.

VI. CONCLUSIONS

The mathematical model, the control strategies and a novel control method for a hybrid active power filter with an injection circuit have been proposed. This control method helps reduce harmonics, has short dynamic response time and effectively improves the total harmonic distortion. It is also useful and applicable to other active filters, especially for nonlinear control systems. Simulation and experimental results demonstrate the effectiveness of the proposed control method.

APPENDIX

Source data:

U=380V, r=0.1Ω; l=0.02mH

PPFs data:

$C_{P1}=264.66\times10^{-6}$ (F); $L_{P1}=0.333\times10^{-3}$(H); R_{P1}=0.023Ω

$C_{P2}=154.38\times10^{-6}$ (F); $L_{P2}=0.408\times10^{-3}$(H); R_{P2}=0.033Ω

Output filter data:

L_0=0.35mH; C_0=60μF

Injection circuit data:

C_F=26.75 μF

Fundamental resonance circuit:

L_1=14.75mH; C_1=690 μF;

Load data:

Thyristor controllable rectifier with L=0.3mH; C=50μF; R_1=3 Ω; (at t=0.6s the THD of the load changes by the regulation enable angle of the rectifier from 0^0 to 30^0 and by using a resistor R_2 in parallel with the resistor R_1; R_2=12 Ω)

Voltage source inverter: C=5000μF

ACKNOWLEDGMENT

The financial support of The National Natural Science Foundation of China (Project No. 60774043) and The National Basic Research Program of China (973 Program) (Project No.2009CB219706) are highly acknowledged.

REFERENCES

[1] F. Peng, H. Akagi, and A. Nabae, "A new approach to harmonic compensation in power system-a combined system of shunt passive and series active filters," *IEEE Trans. Ind. Appl.*, Vol. 26, No. 6, pp. 983-990, Nov./Dec. 1990.

[2] H. Na, H. Lina, W. Jian, and X. Dianguo, "Study on optimal design method for passive power filters set at high voltage bus considering many practical aspects," in *Proc. IEEE 23rd Annu. Applied Power Electronics Conf. Expo*, pp. 396-401, 2008.

[3] L. Gyugyi, and E. C. Strycula, "Active ac power filters," *IEEE IIAS Annual Meeting*, pp. 529-535, 1976.

[4] H. Ming, and C. Heng, "Active power filter technology and its application," *Automation of Electric Power Systems*, pp. 66-70, 2000.

[5] H. Fujita and H. Akagi, "A practical approach to harmonic compensation in power system-series connection of passive and active filters," *IEEE Trans. Ind. Appl.*, Vol. 27, No. 6, pp. 1020-1025, Nov./Dec. 1991.

[6] F. Ruixiang, L. An, and L. Xinran, "Parameter design and application research of shunt hybrid active power filter," *Proc. CSEE*, Vol. 26, No.2, pp. 106-111, Jun. 2006.

[7] L. Malesani, P. Mattavelli, and P. Tomasin, "High performance hysteresis modulation technique for active filters," *IEEE Trans. Power Electron.*, Vol. 12, No. 5, pp. 876-884, Sep. 1997.

[8] Y. Chen, B. Fu, and Q. L. Li, "Fuzzy logic based auto-modulation of parameters PI control for active power filter," *Intelligent Control and Automation, WCICA 2008. 7th World Congress on*, pp. 5228-5232, 2008.

[9] C. Wei, L. Qin, L. Tingjin, R. Penghui , and Z. Yanqing, "Method of event detection based on dynamic hybrid fuzzy logic system," *International Conference on Intelligent Computation Technology and Automation*, pp. 661-663, 2010.

[10] Ahmed A. Helal, Nahla E. Zakzouk, and Yasser G. Desouky, "Fuzzy logic controller shunt active power filter for three-phase four-wire systems with balanced and unbalanced loads," *World Academy of Science, Engineering and Technology*, Vol. 5, No. 8, pp. 621-626, 2009.
[11] C. N. Bhende, S. Mishra, and S. K. Jain, "TS-fuzzy-controlled activepower filter for load compensation," *IEEE Trans. Power Del.*, Vol. 21, No. 3, pp. 1459-1465, Jul. 2006.
[12] A. Hamadi, K. Al-Haddad, S. Rahmani, and H. Kanaan, "Comparison of fuzzy logic and proportional integral controlier of voltage source active filter compensating current harmonics and power factor," *IEEE International Conference on Industrial Technology (ICIT)*, pp. 645-650, 2001.
[13] S. Kerrouche and F. Krim, "Three-phase active power filter based on fuzzy logic controller," *International Journal of Sciences and Techniques of Automatic control & computer engineering IJ-STA*, Vol. 3, No. 1, pp. 942-955, Jul. 2009.
[14] A. Luo, Z. K. Shuai, Z. J. Shen, W. J. Zhu, and X. Y. Xu, "Design considerations for maintaining DC-side voltage of hybrid active power filter with injection circuit," *IEEE Trans. Power Electron.*, Vol. 24, No. 1, pp. 75-84, Jan. 2009.
[15] O. Karasakal, M. Guzelkaya, I. Eksin, and E. Yesil, "Online rule weighting of fuzzy PID controllers," *IEEE International Conference on System Man and Cybernetics (SMC)*, pp. 1741-1747, 2010.
[16] C. Madtharad and S. Premrudeepreechachrn, "Active power filter for three-phase four-wire electric systems using neural networks," *Elect. Power Syst. Res*, Vol. 60, No. 2, pp. 179-192, Apr. 2002.
[17] K. Çağatay Bayındır, M. Uğraş Cuma, and M. Tümay, "Hierarchical neuro-fuzzy current control for a shunt active power filter," *Neural Computing and Applications*, Vol. 15, No. 3, pp. 223-238, 2006.
[18] J.-S. R. Jang, "ANFIS: adaptive-network-based fuzzy inference system," *IEEE Tran.s Syst., Man, Cybern.*, Vol. 23, No. 3, pp. 665-685, May/Jun. 1993.

MinhThuyen Chau was born in Binh Dinh, Vietnam, on June 6, 1977. He received his B.S. and M.S. from the Da Nang University of Technology, Da Nang, Vietnam, and the University of Technical Education Ho Chi Minh City, Ho Chi Minh City, Vietnam, in 2001 and 2005, respectively. Since 2004, he has been a Lecturer at the Ho Chi Minh City University of Industry, Ho Chi Minh City, Vietnam. He is currently pursuing his Ph.D. in the College of Electrical and Information Engineering at Hunan University, Changsha, China. His current research interests include electric power savings, reactive power compensation, and active power filters.

An Luo (Senior Member, IEEE) was born in Chang Sha, China, on July 21, 1957. He received his B.S. and M.S. from Hunan University, Hunan, China, in 1982 and 1986, respectively, and his Ph.D. from Zhejiang University, Zhejiang, China, in 1993. He was with the Central South University, Hunan, China, as a Professor from 1996 to 2002. Since 2003, he has been a Professor at Hunan University. His current research interests include power conversion system, harmonics suppression, reactive power compensation, and electric power savings. He has published over 100 journal and conference articles. He was a recipient of the 2006 National Scientific and Technological Award of China, the 2005 Scientific and Technological Award from the National Mechanical Industry Association of China, and the 2007 Scientific and Technological Award from the Hunan Province of China. He currently serves as the Associate Board Chairperson of the Hunan Society of Electrical Engineering. He also serves as the Chief of the Hunan Electric Science and Application Laboratory.

Zhikang Shuai (Member, IEEE) was born in Shandong, China, on December 19, 1982. He received his B.S. from the College of Electrical and Information Engineering, Hunan University, Changsha, China, in 2001. Since 2005, he has been a graduate student in the College of Electrical and Information Engineering, Hunan University. His current research interests include electric power savings, reactive power compensation, and active power filters. Dr. Shuai was a recipient of the 2007 Scientific and Technological Award from the National Mechanical Industry Association of China.

Fujun Ma was born in Hunan, China, in June, 1985. He received his B.S. and M.S. from the College of Electrical and Information Engineering, Hunan University, Changsha, China, in 2008 and 2010, respectively. Since September 2010, he has been working towards his Ph.D. in the College of Electrical and Information Engineering, Hunan University. His current research interests include power quality managing techniques of electrified railways, electric power savings, reactive power compensation, and active power filters.

Ning Xie was born in Shandong, China, in April, 1988. He received his B.S. from the College of Electrical and Information Engineering, Shandong Jiaotong University, Jinan, China, in 2009. Since 2010, he has been a graduate student in the College of Electrical and Information Engineering, Hunan University, Hunan, China, where he is currently pursuing his Ph.D. His current research interests include power quality managing techniques, electric power savings, active power filters and photovoltaic power stations.

VanBao Chau was born in Binh Dinh, Vietnam, on July 06, 1974. He received his B.S. and M.S. from the University of Technical Education Ho Chi Minh City, Ho Chi Minh City, Vietnam, in 1999 and 2005, respectively. Since 2004 he has been a Lecturer at Ho Chi Minh City University of Industry, Ho Chi Minh City, Vietnam. His current research interests include electric power savings, reactive power compensation, power electronics, and active power filters.